CHINESE OPTICS LETTERS

Vol. 22, No. 5 | May 2024

Preparation of panda-shaped photonic crystal fibers with and without silver wire

Junbo Lou (娄俊波)[1*], Yonghui Yang (杨永辉)[1], Qiang Qu (曲 强)[1], and Shuguang Li (李曙光)[2]

[1] School of Electronic and Information Engineering, University of Science and Technology Liaoning, Anshan 114051, China

[2] State Key Laboratory of Metastable Materials Science & Technology and Key Laboratory for Microstructural Material Physics of Hebei Province, School of Science, Yanshan University, Qinhuangdao 066004, China

*Corresponding author: loujunbo@ustl.edu.cn

Received November 25, 2023 | Accepted January 16, 2024 | Posted Online May 8, 2024

A method of preparing panda-shaped photonic crystal fibers (PCFs) based on secondary drawing technology is proposed in this paper. The secondary drawing can not only reduce fiber diameter but also reduce core size by adding a glass sleeve. Silver-filled and non-silver-filled panda PCFs are prepared. The two ends of silver-filled panda PCF are connected with a broadband light source and a spectrometer, respectively, and the surface plasmon resonance phenomenon is detected. The secondary drawing technology provides a meaningful reference for the preparation of PCF in the future, and the prepared silver-filled panda PCF can be prepared into an optical fiber filter.

Keywords: photonic crystal fiber; secondary drawing technology; air pressure regulation; surface plasmon resonance.
DOI: 10.3788/COL202422.050603

1. Introduction

Photonic crystal fiber (PCF) was first proposed by Philip Russell on the basis of photonic crystal and fiber[1]. According to the different light guiding mechanisms, PCF can be divided into two types: refractive index guided type[2] and photonic band gap type[3]. The cladding of PCF is composed of periodically arranged pores, and the structure of pores can be changed flexibly, so PCF has many excellent characteristics, such as polarization[4], controllable dispersion[5], non-cutoff single-mode transmission[6], high birefringence[7], low limiting loss[8], large mode field area[9], and high nonlinearity[10]. In order to obtain new functional properties, researchers filled the PCF cladding pores with different materials such as gas[11], polymer[12], oil[13], liquid[14], metal[15], and liquid crystal[16].

In recent years, PCF has become a research hotspot, and researchers have made many achievements through their own efforts[17]. Li *et al.*[18] proposed a design method of the PCF polarization filter, which transforms the optimization design problem of the polarization filter into a single objective function optimization problem. By fine-tuning two variables at the same time, this method improves the bandwidth of the polarization filter and achieves higher crosstalk at 1550 nm. Zhou *et al.*[19] proposed a silver-coated D-type PCF plasma sensor. When the silver film thickness is 50 nm, the spectral sensitivity of the sensor is 3191.43 nm/RIU. Guo *et al.*[20] proposed a gold-plated plasma D-type PCF sensor. In the refractive index range of 1.37–1.41, the average wavelength sensitivity is 26,927 nm/RIU, and the maximum amplitude sensitivity is 5059 RIU^{-1}. Liu *et al.*[21] designed a rectangular grid PCF sensor with surface plasmon resonance. The sensor uses the ITO layer as plasma material, and the maximum wavelength sensitivity and amplitude sensitivity are 35,000 nm/RIU and 1120.73 RIU^{-1}, respectively. Nazmul *et al.*[22] proposed an ultra-wide range dual-core PCF plasma refractive index sensor. The sensor prevents oxidation problems by covering the top of the silver with a thin layer of titanium oxide. In the refractive index range of 1.10–1.45, the maximum spectral sensitivity obtained is 24,300 nm/RIU, and the corresponding resolution is 4.12×10^{-6} RIU. Tatiana *et al.*[23] proposed a metal-filled side hole PCF temperature sensor based on whispering gallery modes. By filling the metal indium, the PCF can achieve a maximum temperature sensitivity of 18.72 pm/°C. Dong *et al.*[24] reported a C-type micro-open surface plasmon resonance PCF sensor coated with MoO_2 nanofilm. The average sensitivity of the analyte refractive index of 1.31–1.37 in the *x*-polarization direction is 4821 nm/RIU. Qu *et al.*[25] designed a V-shaped PCF filter with gold film. At the resonance wavelength of 1550 nm, the losses of *x*- and *y*-polarized light are 858 and 68,904 dB/cm, respectively. Because the loss of *y*-polarized light is much greater than that of *x*-polarized light, *y*-polarized light is filtered out at the wavelength of 1550 nm. Liu *et al.*[26] proposed a single-polarization PCF filter based on surface plasmon resonance. At the communication wavelength of 1310 nm, the filtering effect can achieve loss of 588.9 dB/cm, and the corresponding filtering bandwidth is 270 nm. Although researchers have reported many

achievements in PCF, most of them are in theoretical design, and there are very few reports on how to prepare PCF in experiments.

In view of the shortcomings of existing PCF preparation techniques, a method for preparing panda-shaped PCF by combining secondary drawing technology and air pressure control is proposed in this paper. Panda-shaped PCF and silver-filled panda-shaped PCF are prepared by reasonably adjusting fiber drawing parameters, and surface plasmon resonance is detected in the test of silver-filled panda-shaped PCF.

2. Preparation of Panda-Shaped PCF

The main idea of preparing panda-shaped PCF is to use thin-walled capillaries to construct two large circles near the fiber core. Glass tubes with a 20 mm outer diameter and 10 mm inner diameter are drawn into thick-walled capillaries with a 2 mm outer diameter, and glass tubes with a 20 mm outer diameter and a 14 mm inner diameter are drawn into thin-walled capillaries with a 2 mm outer diameter. Thick-walled capillary tubes are stacked into a hexagon with a three-layer structure by a stacking method. The central capillary is replaced with a 2 mm diameter solid capillary rod, and the two thick-walled capillaries adjacent to the fiber core in the horizontal direction are replaced with two thin-walled capillaries. Finally, the stacked hexagonal structure is inserted into a glass sleeve with an outer diameter of 20 mm and an inner diameter of 14 mm, and the gap between the hexagonal structure and the glass sleeve is filled with fine solid capillary rods of different sizes, as shown in Fig. 1(a). Because the inner diameter of the high temperature furnace in the laboratory is 25 mm, the core size cannot be reduced to less than 10 μm by the primary drawing, so the panda-shaped PCF is prepared by the secondary drawing method. The so-called secondary drawing method refers to drawing twice. The thick preform is drawn into a thin preform in the primary drawing. After that, the thin preform is added to a glass outer sleeve for secondary drawing, which can not only reduce the outer diameter size but also the fiber core size. Because the primary drawing has solidified the internal structure of PCF, the secondary drawing can better eliminate the brattling of PCF during drawing and maintain the integrity of PCF. In the primary drawing, the initial furnace temperature is set to 1980°C. After the first dropper falls, the furnace temperature is set to 1810°C, the rod feeding speed is set to 4 mm/min, and the traction speed is set to 0.5 m/min. No external air pressure is needed in the primary drawing process. When the furnace temperature and rod feeding speed are gradually reduced to 1778°C and 1.7 mm/min, respectively, and the drawing speed is gradually increased to 2.9 m/min, the thick preform with a diameter of 20 mm is drawn into a thin preform with a diameter of 3.1 mm, as shown in Fig. 1(b). From Fig. 1(b), the hexagonal structure is complete, with two large air holes adjacent to the core in the horizontal direction, and small air holes in other positions of the cladding, forming a panda-shaped structure.

The initial furnace temperature during secondary drawing is set to 1950°C, and the furnace temperature is adjusted to 1800°C after the first dropper falls. After the diameter of fiber filaments is stabilized, the furnace temperature is gradually lowered. The purpose of gradually lowering the furnace temperature is to make the cladding pores appear as soon as possible. When the furnace temperature is reduced to 1775°C, all air holes in the cladding appear, and two large air holes appear adjacent to the fiber core, as shown in Fig. 2(a). From Fig. 2(a), there is a crescent-shaped gap between the inner structure of optical fiber and the glass sleeve. In order to prevent the air hole from collapsing and eliminating the crescent-shaped gap, an air pressure control device is added to the end of thin preform, and the air pressure threshold is gradually increased. When the air pressure threshold is 10 kPa, the crescent-shaped gap is eliminated, as shown in Fig. 2(b). In order to reduce the fiber diameter, the rod feeding speed is gradually reduced, and the pulling speed is gradually increased. When the rod feeding speed decreases to 1 mm/min and the pulling speed increases to 1.5 m/min, the fiber diameter decreases to 292 μm. At this time, the two large pores adjacent to the fiber core are squeezed into two orange petal shapes, as shown in Fig. 2(c). Continue to adjust the drawing parameters. When the high-temperature furnace temperature is 1789°C, the rod feeding speed is 0.95 mm/min, the

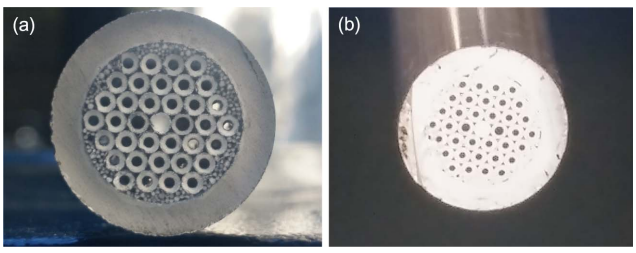

Fig. 1. Panda-shaped PCF preform: (a) panda-shaped PCF thin preform, (b) after the first drawing.

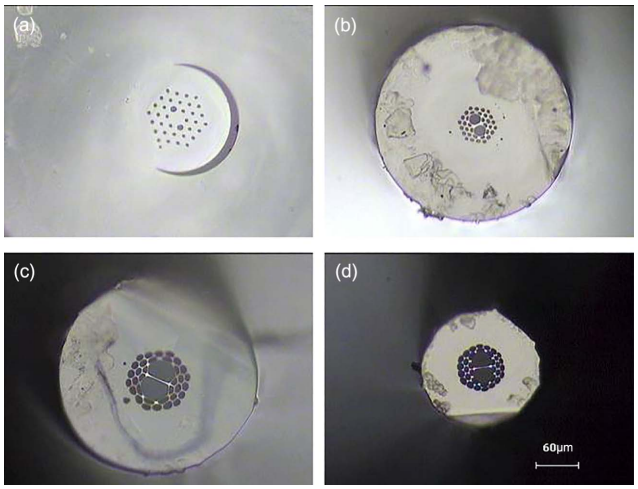

Fig. 2. End view of orange petal-shaped PCF in preparation process: (a) cladding pores appear as a whole, (b) crescent gap disappears, (c) orange petal-shaped pores appear, (d) orange petal-shaped PCF.

pulling speed is 5.9 m/min, and the air pressure threshold is 7 kPa, the fiber diameter is reduced to 125 μm, but the two large air holes adjacent to fiber core are still orange petals, as shown in Fig. 2(d).

The main reason for extruding two big circles into two orange petals is that the wall thicknesses of two kinds of glass tubes are quite different, so in the re-experiment, glass tubes with wall thicknesses of 5 mm and 6 mm are used to draw capillaries. After the first drawing, the thick preform with a diameter of 20 mm is drawn into a thin preform with a diameter of 3.1 mm. The thin preform is loaded into a glass sleeve for secondary drawing. During the secondary drawing process, the furnace temperature is set to 1800°C after the first dropper falls, and then the furnace temperature is sharply reduced. When the furnace temperature is 1750°C, the cladding pores appear as a whole, as shown in Fig. 3(a). At this time, there is a crescent-shaped gap between the inner structure of optical fiber and the glass sleeve. In order to eliminate the gap, an air pressure control device is connected to the tail end of thin preform, and the air pressure threshold is gradually increased. In order to prevent PCF from becoming brittle, the temperature of the high-temperature furnace is gradually increased. When the air pressure threshold is 13.4 kPa and the high-temperature furnace temperature is 1770°C, the crescent-shaped gap is eliminated, and two large pores appear adjacent to fiber core, as shown in Fig. 3(b). In order to reduce the structural size of PCF, the pulling speed is gradually increased, and the rod feeding speed is gradually reduced. The end face of PCF is observed repeatedly by the optical microscope, and the temperature of the high-temperature furnace, air pressure threshold, rod feeding speed, and traction speed are continuously adjusted. When the high-temperature furnace temperature is 1794°C, the air pressure threshold is 10.5 kPa, the rod feeding speed is 1 mm/min, and the pulling speed is 8.1 m/min, the diameter of panda-shaped PCF is reduced to 125 μm, and the fiber core is extruded into an ellipse by two large air holes as shown in Figs. 3(c) and 3(d), in which Fig. 3(c) is an overall end view and Fig. 3(d) is a partially enlarged view.

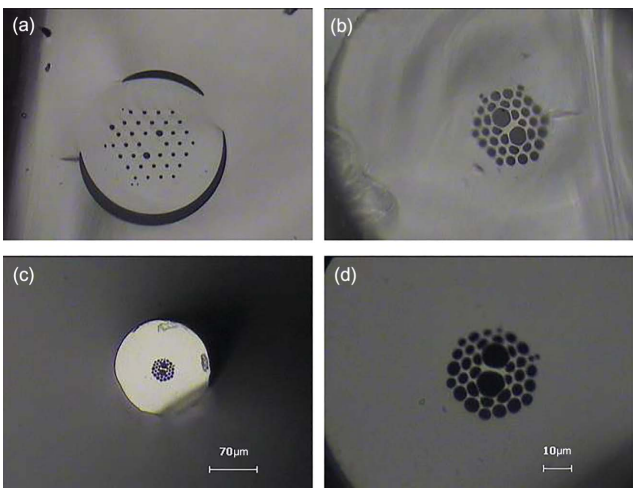

Fig. 3. End view of panda-shaped PCF in preparation process: (a) cladding pores appear as a whole, (b) crescent gap disappears, (c) panda-shaped PCF integral end face, (d) panda-shaped PCF local amplification.

The fitting curve of the temperature and air pressure when drawing panda-shaped PCF is shown in Fig. 4. In order to make the cladding pores appear as soon as possible, during the process of reducing fiber diameter from 1153 to 911 μm, the furnace temperature is sharply reduced from 1800°C to 1750°C. After that, the furnace temperature is gradually increased from 1750°C to 1795°C. The purpose of gradually increasing the furnace temperature is to prevent fiber filaments from becoming brittle and being pulled off during the thinning process. The fitting formula of the temperature and fiber diameter is

$$y = 1861.87932 - 0.80718x + 0.00293x^2 - 5.05564E - 6x^3 + 3.94114E - 9x^4 - 1.10621E - 1x^5. \quad (1)$$

From Fig. 4(b), the air pressure threshold increases from 1 to 14 kPa as the fiber diameter decreases from 1026 to 564 μm. The purpose of raising the air pressure threshold is to eliminate the gap between the inner structure of optical fiber and the glass sleeve. With the fiber diameter decreasing from 564 to 125 μm, the air pressure threshold gradually decreases from 14 to 9.5 kPa. The gradual decrease of the air pressure threshold is to prevent the cladding pores from being squeezed and deformed. The fitting formula between air pressure threshold and fiber diameter is

$$y = 10.24969 - 0.01699x + 1.11721E - 4x^2 - 1.59382E - 7x^3 + 5.75761E - 1x^4. \quad (2)$$

Figure 5 is the fitting curve of the rod feeding speed and pulling speed during the drawing process of panda-shaped PCF. In order to reduce the size of PCF, the rod feeding speed is gradually decreased, while the pulling speed is gradually increased. When the diameter of panda-shaped PCF decreases from 1153 to 564 μm, the rod feeding speed decreases greatly, while the pulling speed basically does not change. When the diameter of panda-shaped PCF decreases from 564 to 125 μm, the rod feeding speed basically does not change, but the pulling speed increases greatly. The fitting formulas of rod feeding speed and pulling speed are as follows:

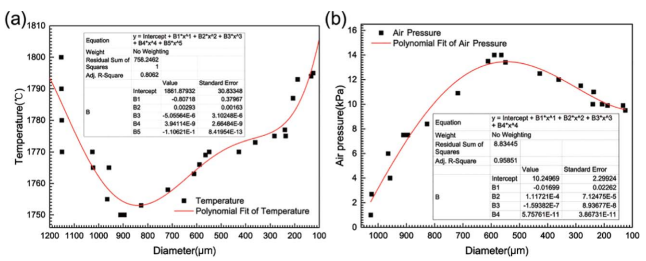

Fig. 4. Fitting curves of (a) temperature parameters and (b) air pressure parameters with fiber diameter during the preparation of panda-shaped PCF.

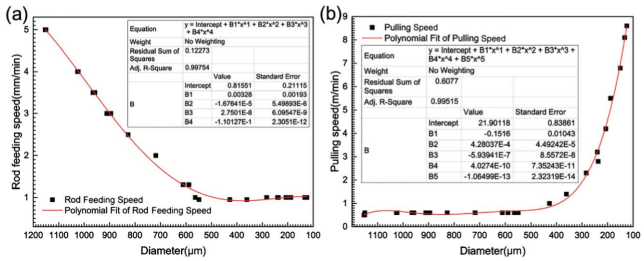

Fig. 5. Fitting curves of (a) rod feeding speed and (b) pulling speed with fiber diameter during the preparation of panda-shaped PCF.

$$y = 0.81551 + 0.00328x - 1.67641E - 5x^2 + 2.7501E - 8x^3 - 1.10127E - 1x^4, \quad (3)$$

$$y = 21.90118 - 0.1516x + 4.28037E - 4x^2 - 5.93941E - 7x^3 + 4.0274E - 10x^4 - 1.06499E - 13x^5. \quad (4)$$

3. Preparation and Testing of Silver-Filled Panda-Shaped PCF

The silver-filled panda PCF preform is prepared by step stacking method. The glass tube with an outer diameter of 20 mm and an inner diameter of 14 mm is drawn into thick-walled capillaries with an outer diameter of 2 mm, and the glass tube with an outer diameter of 16 mm and an inner diameter of 12 mm is drawn into thin-walled capillaries with an outer diameter of 2 mm. A silver wire with a diameter of 1.0 mm is stuffed into a thick-walled capillary. When stacking preforms, the thick-walled capillaries are first stacked into a hexagonal shape, and then the capillary tube in the center is replaced with a solid capillary rod with a diameter of 2 mm, and the capillary at the corresponding position of the second cladding layer is replaced with a silver wire filled capillary, as shown in Fig. 6(a). In Fig. 6(a), the capillary in the darker position is the capillary filled with silver wire. Two thick-walled capillaries adjacent to the fiber core in the horizontal direction are replaced by two thin-walled capillaries. Because of the small difference in wall thickness between thin-walled capillaries and thick-walled capillaries, it is difficult to distinguish them with the right eye. Finally, the hexagonal structure filled with silver wire is stuffed into a glass tube with an outer diameter of 20 mm and an inner diameter of 14 mm, and the gap between the hexagonal structure and the glass sleeve is filled with fine capillary rods with different diameters, so as to form a silver-filled panda-shaped PCF preform. Shooting with flash is shown in Fig. 6(b), where the bright spot is silver wire. After the primary drawing, the silver-filled panda-shaped PCF preform with a diameter of 20 mm is drawn into a thin preform with a diameter of 3.1 mm, as shown in Fig. 6(c). Figure 6(d) is an enlarged two-dimensional end view, from which the existence of silver wire can be clearly seen.

The thin preform after primary drawing is put into a glass tube with an inner diameter of 3.2 mm and an outer diameter of 12 mm for secondary drawing. The fiber filaments drawn at the beginning of the secondary drawing are solid, and the microstructure of cladding pores can appear as a whole after cooling. Figure 7(a) shows the end face of the overall appearance of the cladding pores. From Fig. 7(a), the fiber core and silver wire are relatively large, and their sizes are much larger than those of the surrounding pores. In order to reduce the structure size of optical fiber and prevent the cladding pores from collapsing, the rod feeding speed is gradually reduced, and an air pressure maintaining device is added at the tail end of thin preform. When the rod feeding speed is reduced to 1.5 mm/min and the air pressure threshold is increased to 12.4 kPa, the end face of PCF is shown in Fig. 7(b). In the preparation of silver-filled panda-shaped PCF, the control of the air pressure threshold is very important. If the air pressure threshold is too large in the process of drawing optical fiber, the cladding pores will squeeze and break silver wire, as shown in Fig. 7(c). If the air pressure threshold is too small, the silver wire will become larger, as shown in Fig. 7(d). Therefore, when preparing silver-filled

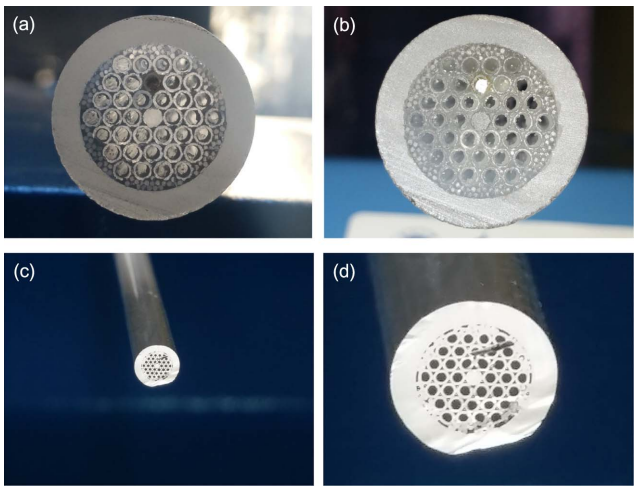

Fig. 6. Silver-filled panda-shaped PCF preform: (a) shooting without flash, (b) shooting with flash, (c) thin preform after the first drawing, (d) local enlargement of thin preform.

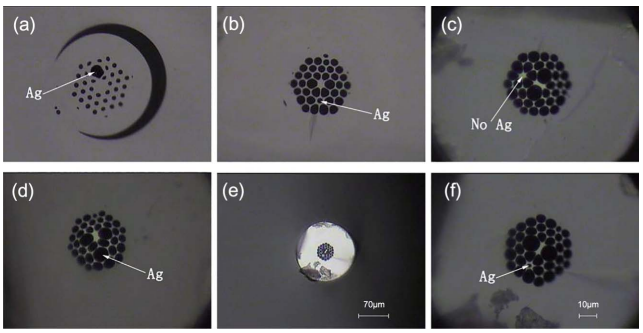

Fig. 7. End face in the process of drawing silver-filled panda-shaped PCF: (a) pores appear as a whole, (b) crescent gap disappears, (c) squeezed silver wire, (d) silver wire supports large pore, (e) silver-filled panda-shaped PCF integral end face, (f) silver-filled panda-shaped PCF local amplification.

panda-shaped PCF, it is necessary to slowly adjust the air pressure threshold to avoid the phenomenon that silver wire is squeezed off or becomes too large. After repeatedly adjusting the drawing parameters, when the furnace temperature is 1798°C, the rod feeding speed is 1 mm/min, the traction speed is 8.9 m/min, and the air pressure threshold is 8.3 kPa, the diameter of the silver-filled panda-shaped PCF is reduced to 125 μm. Under the action of air pressure, the two thin-walled capillaries adjacent to the fiber core become larger, forming two large pores similar to panda eyes. The large pores extrude the fiber core into an ellipse, with a long axis length of about 8 μm and a short axis length of about 3 μm. Under the squeezing action of cladding pores, the size of the silver wire becomes the smallest, as shown in Figs. 7(e) and 7(f), where Fig. 7(e) is the whole end face and Fig. 7(f) is the locally enlarged end face.

Figure 8(a) shows the fitting curve of temperature parameters with the fiber diameter during the preparation of silver-filled panda-shaped PCF. At the beginning of fiber drawing, the cladding pores appear mainly by lowering furnace temperature. Because the filaments are thick at first and are not easily broken, the temperature drops greatly. When the furnace temperature is reduced to 1760°C, almost all cladding pores appear. At this time, an air pressure control device is added at the end of the preform, and the air pressure threshold is gradually increased. Figure 8(b) shows the fitting curve of air pressure parameters during the preparation of silver-filled panda-shaped PCF. As the filament becomes thinner, optical fiber begins to become brittle. In order to prevent optical fiber from being broken, the furnace temperature is gradually raised. In the process of furnace temperature rising, the cladding pores may collapse, so the air pressure threshold should be gradually increased. The fitting formulas of temperature parameters and air pressure parameters are Eqs. (5) and (6), respectively:

$$y = 1890.75672 - 1.02561x + 0.0028x^2 - 3.17607E - 6x^3 + 1.27916E - 9x^4, \tag{5}$$

$$y = 3.42651 + 0.04234x - 4.81743E - 5x^2 + 4.93178E - 10x^3 + 5.5135E - 12x^4. \tag{6}$$

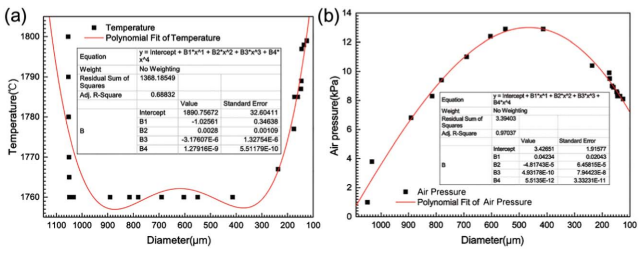

Fig. 8. Fitting curves of (a) temperature parameters and (b) air pressure parameters with fiber diameter during the preparation of silver-filled panda-shaped PCF.

Figures 9(a) and 9(b) show the fitting curves of the rod feeding speed and traction speed. In order to reduce the size of the fiber core, the rod feeding speed should be gradually reduced, while the pulling speed should be gradually increased. From Fig. 9(a), during the process of decreasing the fiber diameter from 1050 to 550 μm, the rod feeding speed decreases greatly. During the process of decreasing the fiber diameter from 550 to 125 μm, the rod feeding speed decreases slightly. The fitting formula between the rod feeding speed and fiber diameter is

$$y = 0.53598 + 0.00658x - 2.97794E - 5x^2 + 4.73925E - 8x^3 - 2.01371E - 1x^4. \tag{7}$$

From Fig. 9(b), in the process of reducing the fiber diameter from 1050 to 550 μm, the traction speed increases slightly. In the process of reducing the fiber diameter from 450 to 125 μm, the traction speed increases greatly. The fitting formula between the traction speed and fiber diameter is

$$y = 30.93011 - 0.26667x + 9.19674E - 4x^2 - 1.52838E - 6x^3 + 1.21901E - 9x^4 - 3.73517E - 1x^5. \tag{8}$$

Comparing the drawing parameters of silver-filled panda-shaped PCF and unfilled silver panda-shaped PCF, it can be found that the setting curves of the furnace temperature are all down first and then up, showing a concave shape. The temperature drops first to make the cladding pores appear as a whole and then rises to prevent optical fiber from being too brittle and being pulled off. The setting curves of the air pressure threshold are first up and then down, showing a convex shape. The collapse of cladding pores can be prevented by applying air pressure. The setting curves of the rod feeding speed gradually decrease, while the setting curves of the traction speed gradually increase, both aimed at reducing the diameter size of optical fiber.

The two ends of the prepared silver-filled panda-shaped PCF are, respectively, connected to a broadband light source and a spectrometer. The wavelength range of the broadband light source is from 1525 to 1610 nm, and the maximum output power is 23 dBm. The experimental system is shown in Fig. 10(a). The light emitted by the broadband light source passes through the silver-filled panda-shaped PCF and enters

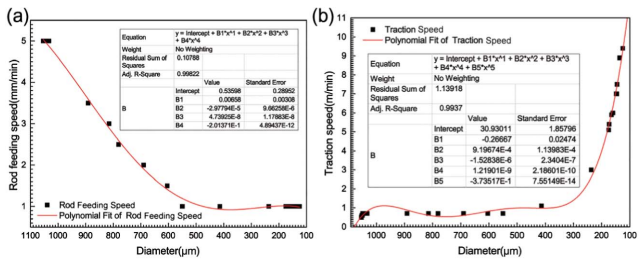

Fig. 9. Fitting curves of (a) rod feeding speed and (b) pulling speed with fiber diameter during the preparation of silver-filled panda-shaped PCF.

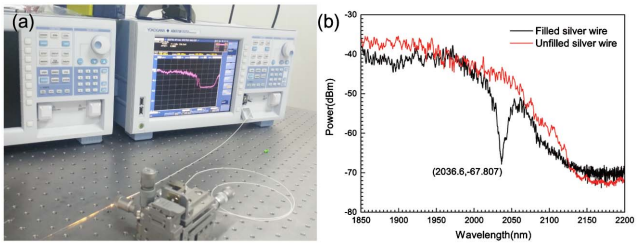

Fig. 10. (a) Silver-filled panda-shaped PCF test experiment and (b) contrast spectrum with or without silver wire.

the spectrometer, and the spectrometer displays the transmission spectrum, as shown in Fig. 10(b). From this transmission spectrum, it can be seen that the transmission spectral power of the silver-filled panda-shaped PCF at the wavelength of 2036.6 nm has a decrease of about 20 dBm, while the transmission spectral power of the unfilled silver panda-shaped PCF at this wavelength does not decrease. This shows that surface plasmon resonance occurs when light waves enter the silver-filled panda-shaped PCF. At the wavelength of 2036.6 nm, the core energy is coupled into the surface of silver wire, so the light wave in this band is filtered out. Therefore, the silver-filled panda-shaped PCF can be used to prepare optical filters.

4. Conclusion

This paper proposes a method for preparing panda-shaped PCF based on secondary drawing technology. Panda-shaped PCF preforms are piled up by capillaries with different wall thicknesses. By filling the capillary with silver wire, the silver-filled panda-shaped PCF preform is prepared. The internal structure of panda-shaped PCF is solidified by the first drawing. During the secondary drawing process, air pressure control is adopted, which not only suppresses the problem of pore collapse in fiber cladding but also generates pores of different sizes in thin-walled and thick-walled capillaries. By adjusting the drawing parameters reasonably, when the furnace temperature is 1794°C, the rod feeding speed is 1 mm/min, the traction speed is 8.1 m/min, and the air pressure threshold is 10.5 kPa, the panda-shaped PCF is prepared. The fiber core is squeezed by two large pores to form an ellipse, and the long axis and short axis of the ellipse are 8 μm and 3 μm, respectively. When the furnace temperature is 1798°C, the rod feeding speed is 1 mm/min, the traction speed is 8.9 m/min, and the air pressure threshold is 8.3 kPa, the silver-filled panda-shaped PCF is prepared. The two ends of silver-filled panda-shaped PCF are connected with a broadband light source and a spectrometer, respectively, and the surface plasmon resonance is detected at the wavelength of 2036.6 nm.

Acknowledgements

This work was supported by the University of Science and Technology Liaoning Talent Project (No. 6003000288) and the National Key Research and Development Program of China (No. 2019YFB2204001).

References

1. P. Russell, "Photonic crystal fibers," Science **299**, 358 (2003).
2. B. Tan, X. W. Chen, and S. C. Li, "Total internal reflection photonic crystal fiber," J. Optoelectron. Laser **13**, 491 (2002).
3. J. Z. Li, H. Peter, V. Christopher, *et al.*, "Colloidal photonic crystal cladded optical fibers: towards a new type of photonic band gap fiber," Opt. Express **13**, 6454 (2005).
4. H. Y. Fu, H. Y. Tam, L. Y. Shao, *et al.*, "Pressure sensor realized with polarization-maintaining photonic crystal fiber-based Sagnac interferometer," Appl. Opt. **47**, 2835 (2008).
5. H. Lim, F. Ilday, and F. Wise, "Femtosecond ytterbium fiber laser with photonic crystal fiber for dispersion control," Opt. Express **10**, 1497 (2002).
6. T. A. Birks, J. C. Knight, and P. S. Russell, "Endlessly single-mode photonic crystal fiber," Opt. Lett. **22**, 961 (1997).
7. T. J. Yang, L. F. Shen, Y. F. Chau, *et al.*, "High birefringence and low loss circular air-holes photonic crystal fiber using complex unit cells in cladding," Opt. Commun. **281**, 4334 (2008).
8. K. Tajima, J. Zhou, K. Nakajima, *et al.*, "Ultralow loss and long length photonic crystal fiber," J. Lightwave Technol. **22**, 7 (2004).
9. K. Saitoh, T. Murao, L. Rosa, *et al.*, "Effective area limit of large-mode-area solid-core photonic bandgap fibers for fiber laser applications," Opt. Fiber Technol. **16**, 409 (2010).
10. M. Musideke, J. Q. Yao, Y. Lu, *et al.*, "High birefringence and high nonlinear octagonal photonic crystal fiber with low confinement loss," Infrared Laser Eng. **42**, 3373 (2013).
11. M. G. Quan, J. J. Tian, and Y. Yao, "Ultra-high sensitivity Fabry–Perot interferometer gas refractive index fiber sensor based on photonic crystal fiber and vernier effect," Opt. Lett. **40**, 4891 (2015).
12. W. Su, S. Q. Lou, H. Zou, *et al.*, "Design of a highly nonlinear twin bow-tie polymer photonic quasi-crystal fiber with high birefringence," Infrared Phys. Technol. **63**, 62 (2014).
13. Y. Geng, L. Wang, Y. Xu, *et al.*, "Wavelength multiplexing of four-wave mixing based fiber temperature sensor with oil-filled photonic crystal fiber," Opt. Express **26**, 27907 (2018).
14. Y. Zhang, C. Shi, C. Gu, *et al.*, "Liquid core photonic crystal fiber sensor based on surface enhanced Raman scattering," Appl. Phys. Lett. **90**, 193504 (2007).
15. S. Y. Zhang, X. Yu, Y. Zhang, *et al.*, "Theoretical study of dual-core photonic crystal fibers with metal wire," IEEE Photonics J. **4**, 1178 (2012).
16. D. D. Wang, G. X. Chen, and L. L. Wang, "Thermal tunability of photonic bandgaps in liquid crystal filled polymer photonic crystal fiber," Opt. Fiber Technol. **29**, 95 (2016).
17. A. A. S. Falah, W. R. Wong, and F. R. M. Adikan, "Single-mode eccentric-core D-shaped photonic crystal fiber surface plasmon resonance sensor," Opt. Laser Technol. **145**, 107474 (2022).
18. H. W. Li, H. L. Chen, Y. X. Li, *et al.*, "Reverse-designed photonic crystal fiber-based polarization filter with optimal performance," Opt. Laser Technol. **168**, 109909 (2023).
19. C. Zhou, H. K. Zhang, P. Song, *et al.*, "D-shaped photonic crystal fiber plasmon sensors based on self-reference channel," IEEE Photon. Technol. Lett. **32**, 589 (2020).
20. Y. Guo, J. S. Li, X. Y. Wang, *et al.*, "Highly sensitive sensor based on D-shaped microstructure fiber with hollow core," Opt. Laser Technol. **123**, 105922 (2020).
21. Q. Liu, J. D. Sun, Y. D. Sun, *et al.*, "Surface plasmon resonance sensor based on photonic crystal fiber with indium tin oxide film," Opt. Mater. **102**, 109800 (2020).
22. H. Nazmul, M. Masuk, H. Faruque, *et al.*, "Dual core photonic crystal fiber based plasmonic refractive index sensor with ultra-wide detection range," Opt. Express **31**, 26910 (2023).

23. T. Muoz-Hernandez, E. Reyes-Vera, and P. Torres, "Temperature sensor based on whispering gallery modes of metal-filled side-hole photonic crystal fiber resonators," IEEE Sens. J. **20**, 9170 (2020).
24. J. Y. Dong and S. H. Zhang, "Characteristics of MoO_2 deposited C-shaped photonic crystal fiber sensor with a micro-opening based on surface plasmon resonance," Plasmonics **18**, 1971 (2023).
25. Y. W. Qu, J. H. Yuan, X. Zhou, *et al.*, "A V-shape photonic crystal fiber polarization filter based on surface plasmon resonance effect," Opt. Commun. **452**, 1 (2019).
26. Y. D. Liu, X. L. Jing, S. G. Li, *et al.*, "Design of a single-polarization filter based on photonic crystal fiber with gold film on the inner wall of two ultra-large holes," Opt. Laser Technol. **114**, 114 (2019).